Aerosol and Air Quality Research, 14: 237–250, 2014

ISSN: 1680-8584 print / 2071-1409 online
doi: 10.4209/aaqr.2013.01.0020

Characterization of $PM_{2.5}$ Major Components and Source Investigation in Suburban Hong Kong: A One Year Monitoring Study

X.H. Hilda Huang[1], Qijing Bian[2], Wai Man Ng[1], Peter. K.K. Louie[3], Jian Zhen Yu[1,2*]

[1] *Environmental Central Facility, Institute of Environment, the Hong Kong University of Science & Technology, Clear Water Bay, Kowloon, Hong Kong, China*
[2] *Department of Chemistry, the Hong Kong University of Science & Technology, Clear Water Bay, Kowloon, Hong Kong, China*
[3] *Hong Kong Environmental Protection Department, 47/F, Revenue Tower, 5 Gloucester Road, Wan Chai, Hong Kong, China*

ABSTRACT

$PM_{2.5}$ filter sampling was conducted on a daily basis at the HKUST Air Quality Research Supersite (AQRS) for one year from March 2011 to February 2012. Approximately one fifth of the filter samples were subjected to full chemical analysis including major ions, elements, organic carbon (OC), elemental carbon (EC), and non-polar organic compounds (NPOCs). The major ions (sulfate, nitrate, and ammonium) were compared with those measured online by a MARGA system and the two sets of data were found in agreement within 25% or better. The major $PM_{2.5}$ components (crustal materials, organic matter, soot, ammonium sulfate, ammonium nitrate, and non-crustal trace elements) accounted for 90% of the measured mass with sulfate being the most abundant (32.0%), followed by organic matter (23.5%) and ammonium (11.8%). The monthly variation patterns for different components suggested variable regional/super-regional sources, reflecting variation of transport contribution caused by shifts in synoptic weather conditions.

Receptor modeling analysis by Positive Matrix Factorization revealed that secondary sulfate formation process (annual average of 31%), biomass burning (23%), and secondary nitrate formation process (13%) were the three dominant contributing sources to the observed $PM_{2.5}$ at HKUST AQRS throughout the sampling year. The $PM_{2.5}$ mass concentrations of all the individual sampling days were within the recently-proposed AQOs standards by the Hong Kong government (35 μg/m^3 for annual average and 75 μg/m^3 for 24-hr average) while approx. 52% of the sampling days were recorded with $PM_{2.5}$ concentrations exceeding the WHO health 24-hr standards of 25 μg/m^3. Major composition and source analysis showed that the increased mass concentrations on high PM days were mainly caused by air pollutant transport from the outside-Hong Kong regions. Results from this study indicate the importance of regional/super-regional strategies such as reduction in SO_2, NO_2 (precursors for secondary inorganic aerosols) and restricting biomass burning for lowering $PM_{2.5}$ in Hong Kong.

Keywords: $PM_{2.5}$ chemical characteristics; $PM_{2.5}$ sources; Regional/Super-regional Transport; Chinese aerosols; MARGA.

INTRODUCTION

Atmospheric aerosols are a highly variable component of the lower atmosphere and play important roles in environmental issues related to global and regional climate, air quality, visibility degradation, chemistry of the atmosphere, and human health effect. Aerosols affect the climate directly by altering the amount of solar radiation reaching the earth's surface, and indirectly by acting as cloud condensation nuclei or altering cloud particle size and number. Aerosols are also closely related to the visibility problems by scattering and absorption of solar radiation. Furthermore, portions of fine particles have the ability to penetrate deep into the human lungs and cause health problems (Novakov and Penner, 1993; Ramanathan *et al.*, 2001; Kanakidou *et al.*, 2005).

Constituents of atmospheric aerosols can be differentiated as inorganic and organic portions according to their chemical properties. The inorganic ionic species in the aerosol (mainly sulfate, nitrate, and ammonium) has been well studied. Other inorganic species include silicates and metal oxides, which come from soil dust and crustal materials. The organic part of the aerosol, on the other hand, covers a very wide range of organic species. The knowledge of the organic

* Corresponding author.
Tel.: (852) 2358 7389; Fax: (852) 2358 1594
E-mail address: jian.yu@ust.hk

aerosols is far from being complete due to instrumental limitations as well as the wide diversity of the organic materials in their molecular structures, physical and chemical properties.

In the past two decades, it has been recognized that organic material is a major component of atmospheric aerosol, contributing 20–60% to the fine aerosol mass in urban environments (Saxena and Hildemann, 1996; Putaud *et al.*, 2004; Zhang *et al.*, 2007) and as high as 90% in rural and remote areas (Andreae and Crutzen, 1997; Roberts *et al.*, 2001; Zhang *et al.*, 2007). Although the molecular compositions of organic aerosols are not well understood, emerging evidence reveals that organic aerosols play important roles in health effect, direct and indirect aerosol forcing, acid-rain chemistry, and visibility impairment.

Aerosols can also be differentiated as primary or secondary according to their sources and formation pathways. Primary aerosols refer to those that are emitted directly in particulate form from sources and the major sources include incomplete fuel combustion, biomass burning, vehicle exhausts, residential cooking, and bioaerosols (e.g., bacteria, fungi, debris from the plant). Many volatile species emitted into the atmosphere undergo oxidation to yield products which have lower volatility and subsequently partition into particle phase. Such particles are considered as secondary aerosols. Identifying aerosol sources and quantifying the relative contributions of different emission sources and secondary formation processes is an essential initial step of air quality management. The Hong Kong Air Pollutants Emission Inventory for 2011 shows the emission sources for respirable particulate matter (PM_{10}) include navigation (37.1%), road transport (19.0%), public electricity generation (16.0%), non-combustion sources (e.g., quarrying, cooking fumes, dust, 15%), other fuel combustion (e.g., industrial, commercial and domestic applications, 12.0%) and civil aviation (0.93%) (HKEPD, 2013). The major emission sources for $PM_{2.5}$ in the PRD region include industrial sources (43.1%), on-road automobiles (36.3%) and power plants (18.7%). There are also some other sources such as navigation (1.8%), biomass burning (1.5%), residential fuel combustion (1.2%) and waste incineration (< 0.1%) (Zheng *et al.*, 2009). While the emission inventory data provide information in identifying major industry sectors contributing to pollution, this information needs to be assessed by source apportionment based on ambient measurements. The latter also provides an estimate of contributions from secondary formation processes. This paper reports results of ambient measurements and subsequent source apportionment.

The ambient concentration and composition of $PM_{2.5}$ are highly dependent on multiple factors including emission sources, atmospheric chemistry, and meteorological conditions. An intensive sampling campaign was conducted at an air quality research supersite located in a suburban area of Hong Kong for one year. The supersite can be used as a background site since there are no heavily traveled roads or other major stationary sources within 2 km of the site. Consequently, most of the pollutants observed at this site are believed to be transported from either downtown Hong Kong or more distant urban areas outside the Hong Kong region, making this supersite a suitable place to study the influence of regional/super-regional transport of air pollutants on Hong Kong. The current study aims to characterize and assess the major chemical composition of the collected $PM_{2.5}$ samples during a one-year period, discern the underlying chemistry, and investigate the dominant contributing emissions sources.

METHODOLOGY

Sampling

The HKUST Air Quality Research Supersite (AQRS) (http://envr.ust.hk/supersite/) is located in a clean suburban area with little residential and commercial development on the east coast of Sai Kung, Hong Kong (22.33°N, 114.27°E). The supersite facility was built on the roof of the seawater pump house on the shorefront (approx. 14 m above sea level) on the campus of the Hong Kong University of Science and Technology, facing Port Shelter and Sai Kung. Similar to the other parts of Hong Kong, the sampling site is mainly under the influence of southerly winds during summertime, north-easterlies during winter, while spring and autumn are transitional seasons in between (Hong Kong Observatory, 2013). The AQRS facility has been put in use since 2011 and the first Hong Kong Air Quality Supersite Study was launched in the spring of 2011. The Automatic Weather Station (AWS) conducts continuous measurements of meteorological parameters including wind speed/direction, temperature, relative humidity, sea level pressure, irradiance and rainfall. The $PM_{2.5}$ sampling using both high-volume and mid-volume samplers was conducted on a daily basis from March 1, 2011 to February 29, 2012.

High-volume $PM_{2.5}$ ambient air samplers (Tisch Environmental Inc., OH, USA) were used to collect 24-hr high-volume $PM_{2.5}$ samples on pre-baked 8 × 10' quartz fiber filters at a flow rate of 40 CFM (approx. 1.13 m^3/min). Speciation Air Sampling Systems (SASS, Met One Instrument, Inc., OR, USA) were used to collect 24-hr mid-volume $PM_{2.5}$ samples at a flow rate of 6.7 LPM. Four channels of the sampler were used to capture the $PM_{2.5}$, one on Teflon filter (47 mm, PALL Life Sciences, MI, USA), one on pre-cleaned Nylon filter (47 mm, PALL Life Sciences, MI, USA) preceded by a MgO-coated denuder, and two on pre-baked quartz fiber filters (47 mm, PALL Life Sciences, MI, USA). No back-up filters were used in this study hence the OC sampling artifacts were not evaluated. Considering the relatively lower levels of both volatile organic compounds (VOCs) and OC in the sampling area, the carbon concentration biases caused by the organic vapor adsorption are not expected to be significant. After the sample collection, all the 47-mm filters were stored in Petri dishes (lined with aluminum foil for quartz fiber filters) and sealed with parafilm. The 8 × 10 inch quartz fiber filters were folded in half and stored in aluminum foil. Filters were refrigerated under 4°C before chemical analysis.

The Teflon filter was used for gravimetric and elemental analysis, Nylon filter for ion analysis, and quartz fiber filter for the analysis of OC and EC. Filter punches from

the high-volume samples were utilized for analysis of non-polar organic compounds (NPOCs) by a thermal desorption-GC/MS technique. Field blanks were collected at the end of each month and were analyzed in parallel to the exposed filter samples as a part of QA/QC procedure (Chow and Watson, 1998).

Gravimetric and Chemical Analyses

$PM_{2.5}$ mass concentration was determined gravimetrically by weighing the Teflon filters before and after sampling using a digital balance (Sartorius AG, Model MC 5-0CE, Göttingen, Germany, capacity of 0.1 mg–5.1 g with a sensitivity of ± 1 μg) in the ENVF weighing facility at HKUST. Prior to weighing, filters were equilibrated in a controlled weighing chamber (24-hr mean temperature in the range of 20–23°C and controlled within ± 2°C, 24-hr mean RH in the range of 30–40% and controlled within ± 5%) for at least 24 hours before and after weighing.

Following the sampling schedule of the PM monitoring network in Hong Kong, one sixth of the collected daily samples were chosen for gravimetric and chemical analyses (major ions, OC, EC, elements and NPOCs). Since four intensive sampling campaigns took place in May, August, November 2011 and February 2012 as the first Hong Kong Air Quality Supersite Study, one third of the daily filter samples collected during these four months were analyzed in particular while other filters are archived.

Water soluble ions, Na^+, NH_4^+, K^+, Mg^{2+}, Ca^{2+},Cl^-, NO_3^-, SO_4^{2-}, and $C_2O_4^{2-}$ were extracted from the Nylon filters using double de-ionized water from the Ultrapure Water System (Nanopure Diamond UV/UF, Barnstead, USA). Chemical analyses of the water-soluble ions were carried out using an Ion Chromatograph (IC) (Dionex DX-500, Thermo Fisher Scientific, MA, USA).

OC and EC were analyzed using thermal/optical transmittance (TOT) method on an Aerosol OCEC analyzer (Sunset Laboratory, OR, USA). The analysis protocol follows the ACE-Asia protocol (Schauer *et al.*, 2003), which is a variant of NIOSH protocol (Wu *et al.*, 2012).

Measurements of elements from Sodium to Uranium were carried out on aerosol deposit on Teflon filters using an energy dispersive X-ray fluorescence (ED-XRF, Epsilon 5, PANalytical, The Netherlands). The accuracy of the XRF measurements have been determined in the ENVF lab at HKUST by comparing results with the certified values of the NIST SRM 2783 (Air Particulate on Filter Media). The measured values for 13 elements (Al, Ca, Cr, Cu, Fe, K, Mg, Mn, Na, Ni, Pb, Ti, and Si) are in agreement with the certified values within 12% and 4 elements (V, Zn, Rb, and S) within 25% in agreement with the certified or reference values.

Small portions of high-volume quartz fiber filter samples were used for NPOCs analysis by a thermal-desorption technique on GCMS. Identification was achieved by comparing the mass spectra and retention times of the chromatographic peaks with those of authentic standards. Quantification was based on peak area ratios of select fragment ions characteristic of individual NPOCs to those of internal standards (Ho *et al.*, 2008).

Other Datasets

The HKUST AQRS facility is also equipped with several real-time instruments in addition to the filter-based PM samplers. The real-time instruments for PM measurements include: (1) a SHARP 5030 Monitor (Thermo Scientific Inc., MA, USA), which continuously measures the $PM_{2.5}$ mass concentrations; (2) a Model-4 Semi-Continuous OCEC Field Analyzer (RT-OCEC) (Sunset Laboratory, OR, USA), which measures hourly OC and EC concentrations; (3) a MARGA (Metrohm Applikon, The Netherlands), which measures the concentration of inorganic species in $PM_{2.5}$ and their related gas-phase components in the ambient air; and (4) an Aerosol Mass Spectrometer (AMS, Aerodyne Research Inc., MA, USA), which quantitatively measures the size and chemical mass loading in real-time for non-refractory sub-micron aerosol particles.

Datasets obtained from the aforementioned SHARP monitor, RT-OCEC, and MARGA were used for comparisons with the results of filter-based measurements. These inter-comparisons among different independent datasets serve as part of the data validation processes and would provide invaluable information for the future studies on atmospheric chemistry and properties of gaseous pollutants and PM.

RESULTS AND DISCUSSION

Data Validation

Three levels of data validation were performed on the dataset acquired from this study. Level I validation mainly includes flagging measurements for deviations from procedures and identifying invalid values. Level II validation examines the internal consistency among different data and attempts to resolve discrepancies based on known physical relationships between variables. This stage of data validation involves comparing a sum of measured chemical species to mass concentration, comparing relevant measurements from different methods, calculating ammonium and charge balances, reconstructing the mass concentration through major PM composition, and examining time series data to identify and investigate outliers. Level III validation is part of the data interpretation process, mainly focusing on identification of unusual values through parallel consistency tests with other independent datasets. In all cases, a Deming linear least-squares regression was used (Deming, 1943; Cornbleet and Gochman, 1979). Deming regression assumes that the uncertainties in both of the datasets are equal while conventional linear least-squares regression only considers the uncertainties in the dependent variable.

Fig. 1 shows the sum of chemical species plotting against the measured $PM_{2.5}$ mass on Teflon filters. The chemical species include those that were quantified on Teflon, Nylon, and quartz fiber filters. To avoid double counting, chloride (Cl^-), water-soluble potassium (K^+) and sodium (Na^+), and sulfate (SO_4^{2-}) are included in the sum while total sulfur (S), chlorine (Cl), sodium (Na), potassium (K), oxalate ($C_2O_4^{2-}$, counted in OC) are excluded. Carbon concentration is represented by the sum of organic carbon (OC) and elemental carbon (EC). Unmeasured ions, metal oxides, or

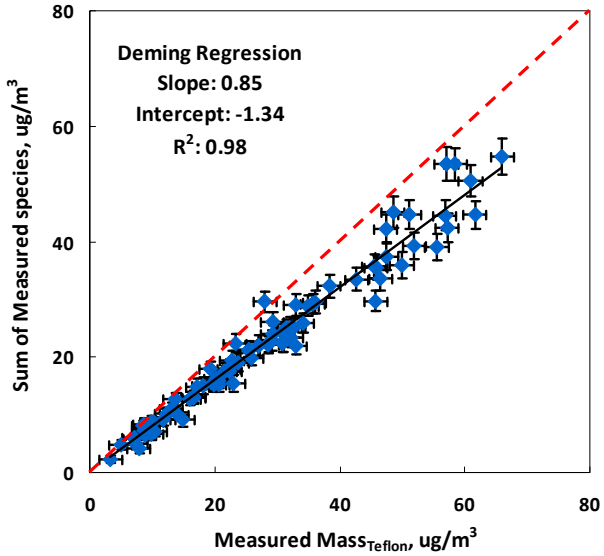

Fig. 1. Scatter plot of sum of measured chemical species versus measured mass on Teflon filter for $PM_{2.5}$ sample collected at HKUST AQRS during Mar. 2011–Feb. 2012.

hydrogen and oxygen associated with OC are not counted into the measured concentrations. Therefore, the sum of the individual chemical concentrations determined for $PM_{2.5}$ samples should be less than the corresponding mass concentrations obtained from gravimetric measurements.

A strong correlation (R^2 = 0.98) was found between the sum of measured species and the measured mass with a slope of 0.85. The average Y/X ratios indicate that around 80% of the $PM_{2.5}$ mass can be explained by the measured chemical species.

SO_4^{2-} and K^+ were measured by IC on Nylon filters while total S and total K were measured by XRF on Teflon filters. The ratio of SO_4^{2-} to S is expected to equal three if all of the sulfur is present as SO_4^{2-}. The ratio of K^+ to K is expected to equal or be less than 1. Fig. 2 shows the scatter plots of (a) SO_4^{2-} versus total S concentrations and (b) K^+ versus total K concentrations. A good correlation (R^2 = 0.96) was observed for SO_4^{2-} vs. total S with a slope of 2.75 and the average sulfate to total sulfur ratio was determined to be 2.45 ± 0.43, which meets the validation criteria (SO_4^{2-}/total S < 3.0). The potassium data comparison showed a bit more scatter (R^2 = 0.94), possibly caused by instrumental and method uncertainties. It is noted that water-soluble potassium was not detected in several samples collected during summer months (e.g., June to August) due to very low PM levels. Hence the ratio of water-soluble potassium to total potassium averages relatively low at 0.73. If these samples were excluded from the dataset, the average ratio of K^+/total K would increase to 0.84 suggesting that most of the total potassium is in its soluble ionic form.

For further validation of the ion measurements, calculated versus measured ammonium (NH_4^+) are compared. NH_4^+ is directly measured by IC analysis of Nylon filter extract. NH_4^+ is very often found in the chemical forms of NH_4NO_3, $(NH_4)_2SO_4$, and NH_4HSO_4 in the $PM_{2.5}$ over Hong Kong (Qin *et al.*, 1997; Ho *et al.*, 2003; Louie *et al.*, 2005a, b; Hagler *et al.*, 2006; So *et al.*, 2007). Assuming full neutralization, measured NH_4^+ can be compared with the computed NH_4^+. Fig. 3 shows the scatter plot of calculated vs. measured NH_4^+ and strong correlations (R^2 = 0.99) can be found for both forms of sulfate while the slopes were quite different (1.05 for ammonium sulfate and 0.62 for ammonium bisulfate). The average ratios of calculated ammonium to measured ammonium suggest that ammonium sulfate is the dominant form for ammonium in the $PM_{2.5}$ observed at HKUST AQRS in the year 2011.

The sum of Cl^-, NO_3^-, SO_4^{2-}, and $C_2O_4^{2-}$ is compared to the sum of Na^+, NH_4^+, K^+, Mg^{2+}, and Ca^{2+} in μeq/m^3 so as to check the charge balance (Fig. 4). The correlation between the anion and cation equivalences was strong (R^2 = 0.99), with a slope of 0.98. The average Y/X ratio is slightly larger than unity since the calculation only accounted for major measured ions and there is a deficiency in cations due to the exclusion of [H^+].

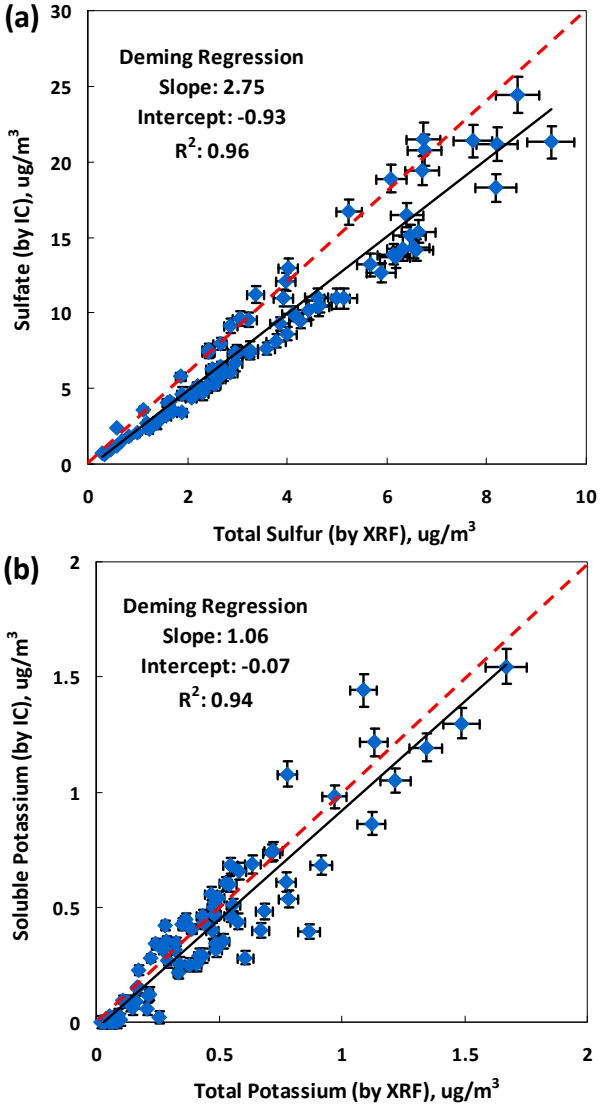

Fig. 2. Scatter plots of (a) SO_4^{2-} vs. total S and (b) K^+ vs. total K for $PM_{2.5}$ samples collected at HKUST AQRS during Mar. 2011–Feb. 2012.

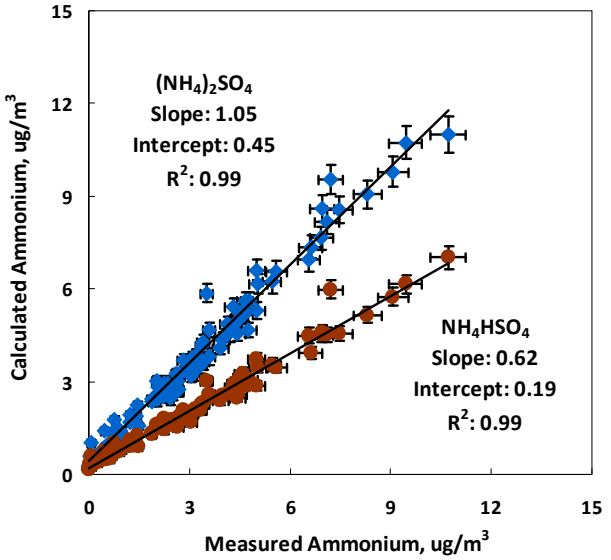

Fig. 3. Scatter plot of calculated ammonium versus measured ammonium for $PM_{2.5}$ samples collected at HKUST AQRS during Mar. 2011–Feb. 2012. The calculated ammonium data are obtained assuming all nitrate was in the form of ammonium nitrate and all sulfate was in the form of either ammonium sulfate (data in blue) or ammonium bisulfate (data in brown).

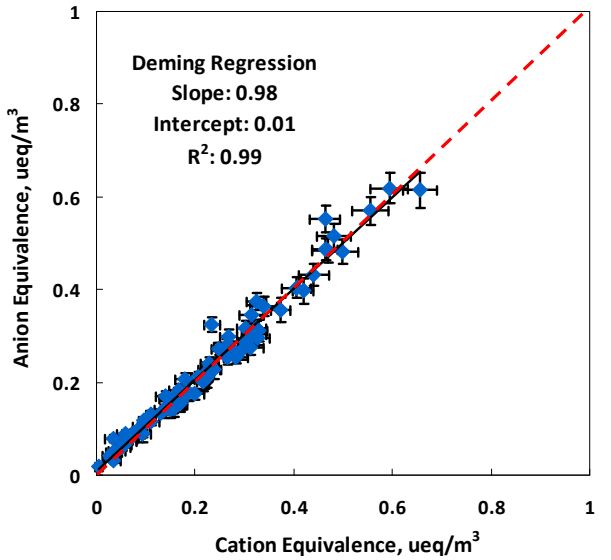

Fig. 4. Scatter plot of anion versus cation measurements for $PM_{2.5}$ samples collected at HKUST AQRS during Mar. 2011–Feb. 2012.

Comparisons were conducted between the dataset obtained from the filter samples in this study and those from three real-time instruments, i.e. $PM_{2.5}$ mass data from SHARP monitor, OC and EC concentrations from RT-OCEC analyzer, and ion data from MARGA (Fig. 5). The Deming linear regression results are also listed in Table 1.

It can be seen from the Deming regression results that good agreements were achieved between real-time and filter-based measurements for most of the species except for EC, Na^+, and K^+. The EC concentrations at the HKUST AQRS were generally low throughout the year (0.86 ± 0.53 μg/m^3). The very low EC loading, from not detected (< 0.06 μgC/cm^2) to 1.75 μgC/cm^2 on the filter in RT-ECOC, caused large uncertainties in instrumental analysis by RT-OCEC, which measured the carbon concentrations on an hourly basis. The more scattered Na^+ data were likely due to the easy contaminations of sodium in filter materials, during sample delivery and during chemical analysis. It is noted that K^+ measured by MARGA was only 60% of those from filter analysis together with a higher degree of scattering than NO_3^-, SO_4^{2-} and NH_4^+. The filter-based measurement results were further compared to the data obtained by the Hong Kong $PM_{2.5}$ monitoring network and fairly good slopes (0.69 for Na^+, 1.10 for NH_4^+, 1.13 for K^+, 1.18 for Cl^-, 2.16 for NO_3^-, 0.99 for SO_4^{2-}, 0.93 for OC and 1.07 for EC, n = 47) and R^2 (0.92 for Na^+, 0.96 for NH_4^+, 0.96 for K^+, 0.69 for Cl^-, 0.94 for NO_3^-, 0.99 for SO_4^{2-}, 0.98 for OC and 0.85 for EC) were found. This result lends credence to the dataset in this study and further investigation is necessary in detailed inspection of the MARGA measurements of K^+. After the Level I and Level II data validations, the valid data percentage of this study is 98.8%.

Reconstruction of $PM_{2.5}$ Mass Concentration and the Temporal Variation

An overall view of the $PM_{2.5}$ major composition can be obtained by combining various measured species into seven components and looking at the percentage contribution of each component to the total fine PM mass. The seven components include 1) crustal material (fine soil); 2) organic matter, which can be estimated from OC concentration by using a multiplier of 1.4; 3) soot, which can be represented by the EC concentration; 4) ammonium sulfate; 5) ammonium nitrate; 6) non-crustal trace elements; and 7) unidentified material. In particular, the crustal component is estimated by summing the soil-associated elements in their oxide form (Al_2O_3, SiO_2, CaO, K_2O, FeO, Fe_2O_3, and TiO_2) (Eldred *et al.*, 1987; Malm *et al.*, 1994; Watson, 2002). The oxide masses were calculated by applying appropriate mass-conversion-factor (mcf) to the measured elements with the following three assumptions: 1) Fe is present as both FeO and Fe_2O_3 and the two forms are equally abundant in molar concentrations; 2) K is also largely generated by nonsoil sources such as biomass burning. Hence, Fe is used as a surrogate for soil-related K by applying [K] = 0.6 [Fe]; and 3) a few minor elements as Na, Mg, C, and S typically contribute 15% to the sediment mass and thus ignored. Therefore, the formula used to calculate the crustal component mass is as below,

$$\text{Crustal material} = 2.2[\text{Al}] + 2.49[\text{Si}] + 1.63[\text{Ca}] + 2.42[\text{Fe}] + 1.94[\text{Ti}] \quad (1)$$

The difference between the reconstructed mass consisting of components 1–6 and the measured mass is referred to as unidentified mass. Considering the large uncertainty in Na measurement by XRF, water-soluble sodium is used in calculation instead of total sodium. Thus,

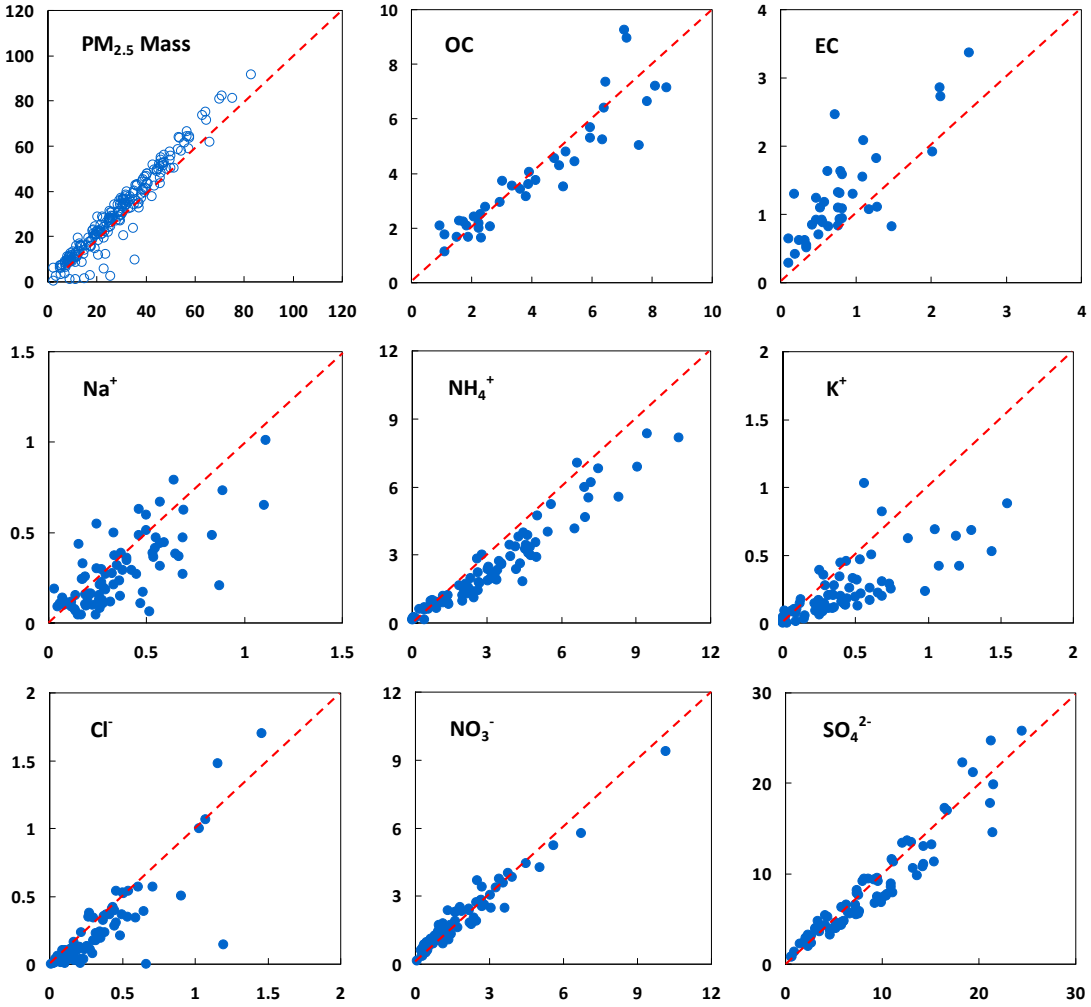

Fig. 5. Scatter plots of real-time measurements versus filter-based chemical data for $PM_{2.5}$ samples collected at HKUST AQRS during Mar. 2011–Feb. 2012. The x-axis represents the species concentrations obtained from filter samples in the unit of μg/m^3. The y-axis represents the 24-hr average species concentrations from real-time measurements (SHARP monitor, RT-OCEC, and MARGA) in the unit of μg/m^3.

Table 1. Results of Deming linear least squares regression of online measurements versus filter-based chemical data including the slope (a), the intercept (b), and the coefficient of determination (R^2).

Species[a]	Deming Linear Least-Squares Regression			
	No. of samples (n)	Slope (a)	Intercept (b)	Coefficient of determination (R^2)
$PM_{2.5}$ mass	225	1.18	–0.41	0.87
OC	39	0.99	–0.21	0.92
EC	39	1.50	–0.03	0.83
Na^+	81	0.86	–0.03	0.61
NH_4^+	81	0.80	–0.51	0.94
K^+	79	0.58	–0.01	0.79
Cl^-	81	1.08	–0.12	0.80
NO_3^-	81	0.76	0.46	0.77
SO_4^{2-}	78	0.99	–1.15	0.70

[a] The online measurements of $PM_{2.5}$ was made by a beta-gauge $PM_{2.5}$ monitor (SHARP 5030), OC and EC by a field aerosol carbon analyzer, and ionic species by a MARGA.

Reconstructed $PM_{2.5}$ mass = [crustal material] + 1.4[OC] + [EC] + [NH_4^+] + [SO_4^{2-}] + [NO_3^-] + [Na^+] + [K] + [Non-crustal trace elements] (2)

The reconstructed mass is plotting against the measured mass in Fig. 6. A strong correlation (R^2 = 0.98) was observed between the reconstructed mass and measured mass and a

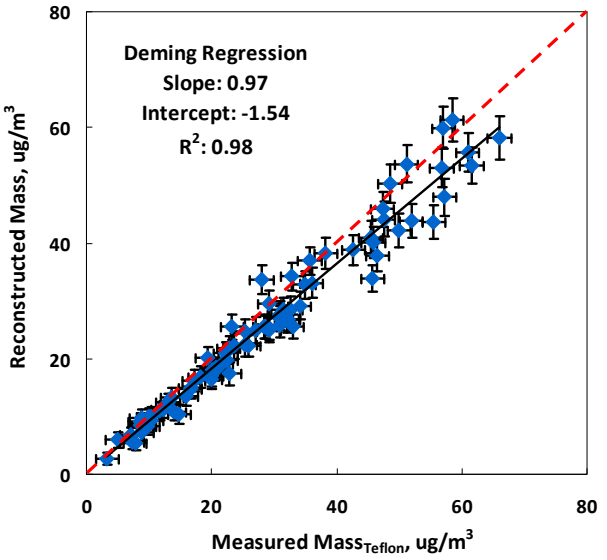

Fig. 6. Scatter plot of reconstructed mass versus measured mass on Teflon filters for $PM_{2.5}$ samples collected at HKUST AQRS during Mar. 2011–Feb. 2012.

slope (0.97) close to unity was obtained. The average Y/X ratio suggests that the reconstructed mass explains approx. 90% of the measured $PM_{2.5}$ mass. One major uncertainty of the reconstructed mass is from the estimation of OM. An empirical value of 1.4 was used as the [OC]-to-[OM] mass conversion factor in this study and it is worth noting that this factor varies with organic aerosol composition. The [OM]/[OC] ratio of freshly emitted aerosols is expected to be smaller than that of the more aging (oxygenated) aerosols.

The monthly average composition of the $PM_{2.5}$ mass is shown in Fig. 7. Sulfate is the most abundant component in the $PM_{2.5}$ mass (32.0% in average, ranging from 24.3–41.1%) followed by OM (23.5% in average, ranging from 14.5–32.8%). Nitrate contributions exhibited a very clear seasonal variation with much higher percentages in winter months (approx. 9.6%) than those in summertime (approx. 4.1%). It is believed that a combination of factors should be responsible for the observed seasonal variation in nitrate concentrations, including the temperature dependence of aerosol nitrate formation (USEPA, 1999) and transport of nitrate from the outside-Hong Kong regions. The lower temperatures in winter months appear to be the driving factor for the higher abundance of nitrate and the elevated influence of transport contribution in winter over summer is consistent with the seasonal change in the prevailing wind directions.

The PM masses contributed by the crustal component were more significant during March and April, 2011. The mass contribution could be as high as 24% of the fine particle mass on individual sampling days during these two months. It is suggested that the elevated crustal-related PM mass was associated with the sandstorms taking place in the northern part of mainland China.

The unidentified mass for $PM_{2.5}$ samples at HKUST AQRS accounts for 0–4.9% (monthly average) of the measured mass. Overall, the reconstructed mass agrees with the measured mass within 10%.

$PM_{2.5}$ Source Apportionment

Positive Matrix Factorization (PMF) analysis was applied to the valid dataset obtained in this study in order to identify major sources to the measured PM mass and estimate their relative contributions in different seasons.

A total of 21 fitting species were selected including $PM_{2.5}$ mass, 8 water-soluble ions (Na^+, NH_4^+, K^+, Mg^{2+}, Cl^-, NO_3^-, SO_4^{2-}, and $C_2O_4^{2-}$), OC, EC, six elements (Al, Si, Ca, V, Fe, and Ni), two PAHs (indeno[*1,2,3-cd*]pyrene and benzo[*ghi*]perylene), and two lumped species characteristic of primary organic aerosol (POA) sources. The two lumped POA species were 1) iso+anteiso, the sum of iso and anteiso-alkanes with carbon number ranging from C_{29} to C_{33}, representing tracers for cigarette smoke (Rogge *et al.*, 1994; Kavouras *et al.*, 1998); and 2) H+S, the sum of five hopane compounds and five sterane compounds, representing tracers for vehicular exhaust (Schauer *et al.*, 1999, 2002). Several other elements (e.g., Ti, Mn and Cu) were not included since these species can be quantified (concentration > LOQ) less than 80% of the time.

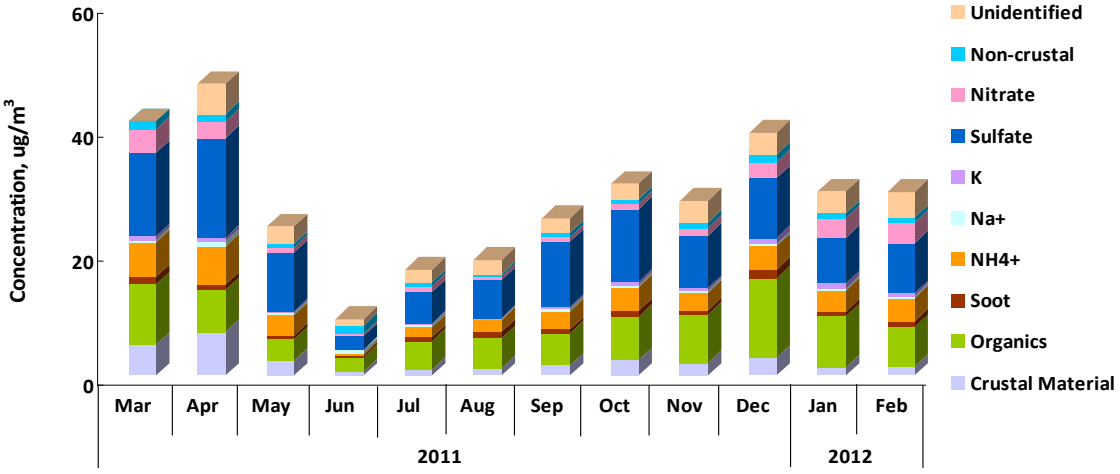

Fig. 7. Monthly average composition of the $PM_{2.5}$ samples collected at HKUST AQRS during Mar. 2011–Feb. 2012.

The uncertainties for individual species were initially estimated as (s_{ij} + MDL_{ij}/3) (Polissar *et al.*, 1998; Reff *et al.*, 2007), where MDL_{ij} is the method detection limit and s_{ij} is the analytical uncertainty of the corresponding species in the dataset. For data which are below the detection limits, the corresponding uncertainty value was set to ((5/6) × MDL_{ij}) (Polissar *et al.*, 1998).

Source apportionment modeling was performed using the USEPA PMF 3.0 software (available at http://www.epa.gov/heasd/products/pmf/pmf.html). This software provides the bootstrap model which is based on the Monta Carlo principle to check the mathematical stability of selected runs (Norris *et al.*, 2008). Each modeling run included 20 base runs and the base run with the minimum Q value was retained as the solution. Solutions for five through ten factors were tested and the eight-factor solution was considered to be the reasonable one. The source profiles of the eight-factor solution are shown in Fig. 8.

The first factor is distinguished by high concentrations of SO_4^{2-} and NH_4^+, suggesting that it is a source associated with the formation of secondary sulfate aerosols. The OC mass apportioned in this factor can also be considered as secondary OC.

The second and seventh factors both have large amounts of Na^+ and Mg^{2+}, which are signatures of sea salt. The difference between the two factors lies in the abundance of Cl^-. "Chloride depletion" occurred during the aerosol aging processes, hence lower chloride level would be expected in aged sea salt particles.

The third factor is distinguished by high concentrations of Al, Si, Ca, and Fe and is suggested to be particles emitted from unpaved roads, construction sites, and wind-blown soil dust. This PMF-derived crustal soil mass is compared with the crustal component calculated in Section 3.2. The Deming linear regression analysis suggests a very good correlation between the two estimations (R^2 = 0.94) and the crustal soil mass by PMF is averagely 78.8% of that by the empirical formula. In addition to the uncertainties of both estimations, the discrepancy would also be caused by the exclusion of Ti in the PMF analysis.

The fourth factor has a high concentration of NO_3^- and is suggested to be associated with the formation of secondary nitrate aerosols. This factor includes a small amount of OC, which is also considered to be secondary OC.

The fifth factor identified by PMF is distinguished by high concentrations of Ni and V, which are well-known indicators for residual oil combustion (Kowalczyk *et al.*, 1982; Chow and Watson, 2002). Hong Kong has one of the world's busiest container terminals located in Kwai Chung, meanwhile HKUST AQRS is on the shorefront facing the Port Shelter and Sai Kung. The vessel emissions could exert influence on the PM mass in the Hong Kong region. The biomass burning-related sources (the sixth factor) are represented by high concentration of the tracer compound K^+. Biomass burning activities are limited in Hong Kong and hence the pollutants generated from these emission sources are postulated to be transported from the outside-Hong Kong regions.

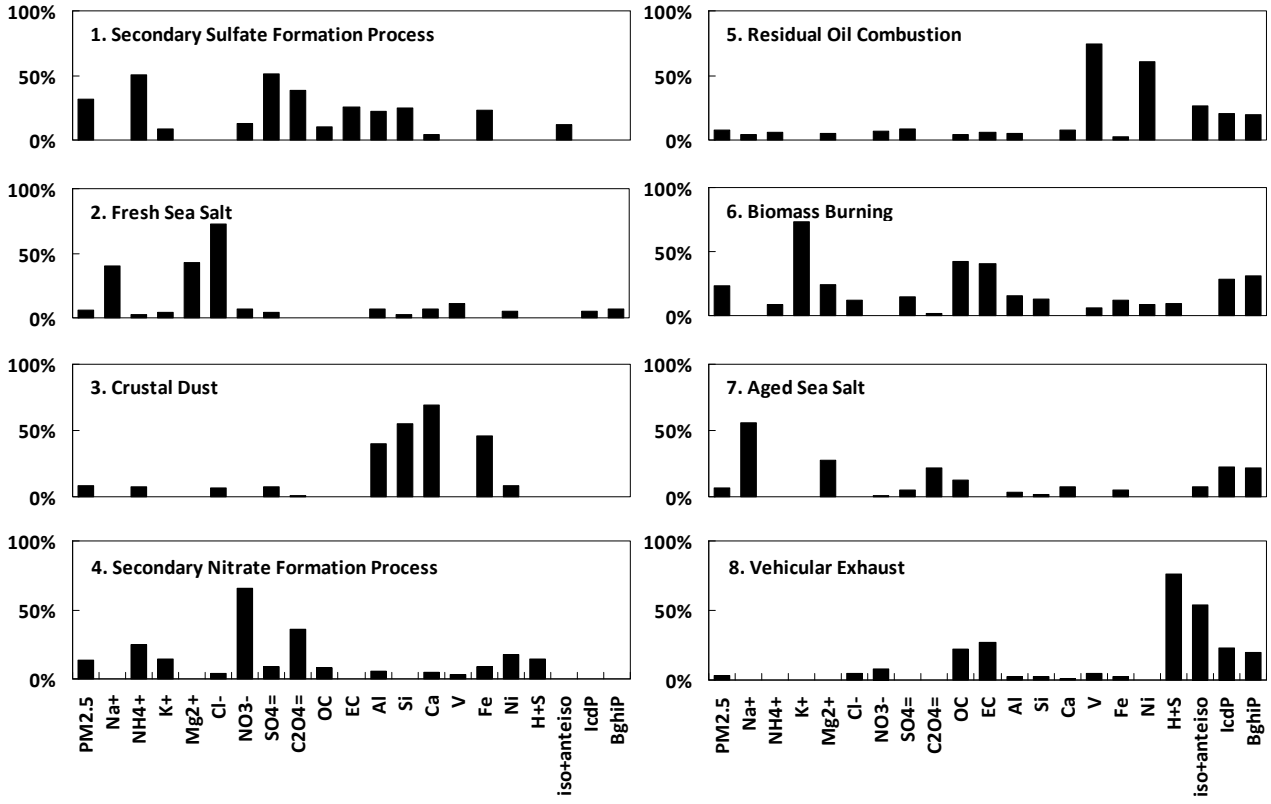

Fig. 8. Source profiles (% of species total) identified by USEPA PMF3.0 for the $PM_{2.5}$ samples collected at HKUST AQRS during Mar. 2011–Feb. 2012.

The eighth factor is characterized by large amount of H+S, iso/anteiso-alkanes, OC and EC, hence suggesting vehicular emission sources. The cigarette smoke source (with iso/anteiso-alkanes as tracers) was unable to be separated from the vehicular exhausts, which is not surprising as smoking in indoor public places has been banned by the HKSAR government so that cigarette smoke activities nowadays are more commonly seen at roadside and the emitted species would be readily mixed with the emissions from automobiles.

The resolved source contributions by PMF are provided in Table 2. On an annual basis, the dominant sources contributing to the $PM_{2.5}$ levels observed at HKUST AQRS are secondary sulfate formation process (31.4%) and biomass burning (22.8%), followed by secondary nitrate formation process (13.4%). The contribution of vehicular exhaust is the least (3.4%) at this suburban site.

We note that a separate secondary OC factor is not resolved by the PMF due to a lack of secondary organic aerosol (SOA) tracers as input species in the PMF analysis. The OC apportioned into factors 1 (secondary sulfate formation process) and 4 (secondary nitrate formation process) is likely secondary, accounting for an annual average of 17.1% of the total OC. A certain amount of secondary OC would be in factors 6 (biomass burning) and 8 (vehicular exhaust). However, due to the lack of SOA tracers specific to vehicular emissions or biomass burning, it is not yet possible to derive the secondary OC portion in these two sources. This result highlights the necessity of more specific SOA marker measurements in order to determine the relative contributions of primary and secondary OC.

Month-to-month variations of the source contributions are shown in Fig. 9. The secondary sulfate formation process consistently contributed quite a lot during most of the time throughout the year except for June 2011, when the prevailing winds were southerly and local emission sources were dominant. This can be explained by the relatively low SO_2 concentrations in the Hong Kong region, meanwhile suggesting that the majority of the sulfate observed were transported from elsewhere. The sea salt sources (both fresh and aged) are important sources throughout the year at HKUST AQRS which is a coastal site. A significant portion contributed by fresh sea salt was found for June and July when the winds mainly came from the sea. On the other hand, the monthly variation of the contribution by aged sea salt was less evident. The sources of residual oil combustion and vehicular exhaust contributed the most during summer months (June to August) while the contribution by crustal dust was significant during March to June. Larger portion of $PM_{2.5}$ was due to the biomass burning-related sources during fall and winter months (~32%) than in the rest of the year, suggesting that these sources are often associated with air pollutants transported from the outside-Hong Kong regions. This result highlights the importance of taking into consideration of biomass burning when modeling regional $PM_{2.5}$ and formulating PM control strategies.

It is noted that little $PM_{2.5}$ mass in October 2011 and a significant more $PM_{2.5}$ mass in November (~2.1 $\mu g/m^3$) was apportioned to the vehicular exhaust factor. An examination of EC distribution among the PMF-resolved factors reveals that most of the EC in October was associated with factors 1 (secondary sulfate formation process) and 6 (biomass burning). Both of these factors are largely related to the non-local sources. The wind data of October and November (not shown) show that the prevailing winds were easterly in October and northwesterly in November. The northwesterly winds would bring in pollutants related to vehicular emissions from the downtown Hong Kong while the easterly winds were more likely associated with pollutant transport from outside-PRD regions. The change in wind direction provides a possible explanation for the significant difference in vehicular emission contribution in the two months. Another factor that could not be ignored is the inherent shortcoming in PMF modeling rooted in using organic tracers for apportioning sources. Hopanes and steranes (i.e., H+S) are used in PMF to identify and apportion contributions by the vehicular exhaust factor. The atmospheric degradation of organic tracers such as hopanes and steranes are known (Yu *et al.*, 2012) but not taken into account in the current PMF model due to lack of knowledge in degradation kinetics and the age of air mass. This could lead to underestimate of the vehicular emission source (e.g., Subramanian *et al*, 2006) and the degree of underestimation would be more prominent for more aged air mass, which might be the case for October 2011.

The relative contributions of sources in local areas (operationally defined as within the Hong Kong region) and non-local regions were estimated based on the source category assignment used by Yuan *et al.* (2012). Sources including vehicular exhaust, residual oil combustion, fresh and aged sea salts are classified as local while secondary sulfate and nitrate formation processes, crustal dust and biomass burning are considered as non-local. Averagely, 34% of the pollutants observed at the HKUST AQRS were generated from the sources within Hong Kong region and 66% were due to the air pollutants transported from the adjacent PRD region or even more distant areas. The contributions from non-local sources maintained at relatively high levels (approx. 76.6%) for 3 out of 4 seasons during the year except for summertime (42.6%). This seasonal variation is consistent with the prevailing wind directions which facilitate the pollutant transport during winter (N and NE) and transitional seasons (spring and fall).

Discussions on High and Low PM Days

The $PM_{2.5}$ standard recommended by the "Air Quality Guidelines" issued by the World Health Organization in 2005 is 25 $\mu g/m^3$ within the 24-hour period of time. By this criterion, 43 out of the 83 sampling days (approx. 52%) in this study exceeded the WHO standard (World Health Organization, 2006). The Hong Kong government announced newly-proposed Air Quality Objectives (AQOs) in January, 2012 and the standards for $PM_{2.5}$ are an annual average of 35 $\mu g/m^3$ and a 24-hour average of 75 $\mu g/m^3$. The $PM_{2.5}$ concentration averaged from the sampling days in this study which cover a one-year time period (27.9 $\mu g/m^3$) did not violate the proposed AQOs annual mean value while none of the individual sampling days recorded the 24-hr average $PM_{2.5}$ level exceeding the AQOs standard,

Table 2. The relative contributions (%) of different emission sources calculated by month, season, and annually from PMF analysis.

% Time Period	Temp. (°C)	RH (%)	$PM_{2.5}$ ($\mu g/m^3$)	Secondary Sulfate Formation Process	Fresh Sea Salt	Crustal Dust	Secondary Nitrate Formation Process	Residual Oil Combustion	Biomass Burning	Aged Sea Salt	Vehicular Exhaust
Mar. 2011	17.1	70.7	38.9	33.4 ± 16.9	4.1 ± 3.3	15.9 ± 11.6	19.6 ± 5.7	1.6 ± 3.1	13.3 ± 6.8	5.1 ± 5.2	7.0 ± 5.0
Apr. 2011	22.0	76.6	47.1	32.2 ± 8.6	8.4 ± 5.6	21.5 ± 9.9	9.8 ± 5.0	5.6 ± 7.8	8.9 ± 4.6	8.6 ± 6.2	5.1 ± 2.8
May 2011	24.3	80.4	24.1	45.1 ± 12.2	3.6 ± 3.1	8.8 ± 7.9	1.9 ± 2.8	20.7 ± 17.1	6.9 ± 7.2	9.0 ± 6.5	4.1 ± 3.4
Jun. 2011	28.5	80.8	9.2	11.6 ± 20.6	30.7 ± 29.7	13.2 ± 10.8	0.0 ± 0.0	18.5 ± 16.0	0.3 ± 1.2	14.1 ± 7.0	11.7 ± 6.6
Jul. 2011	29.0	80.3	17.1	16.3 ± 20.3	26.2 ± 32.6	4.8 ± 3.4	6.0 ± 6.3	23.4 ± 16.5	4.8 ± 5.8	12.3 ± 6.2	6.3 ± 3.8
Aug. 2011	29.8	76.1	18.6	26.3 ± 21.1	7.6 ± 11.3	3.9 ± 4.4	1.1 ± 2.4	36.3 ± 22.8	6.5 ± 8.1	8.6 ± 4.3	9.8 ± 7.0
Sep. 2011	28.0	78.5	25.4	45.2 ± 19.3	11.3 ± 14.1	2.9 ± 1.6	3.2 ± 4.5	5.7 ± 3.2	19.3 ± 12.6	10.9 ± 10.5	1.4 ± 2.2
Oct. 2011	24.6	77.7	31.0	41.7 ± 2.6	3.5 ± 2.4	5.6 ± 2.5	4.1 ± 2.4	3.5 ± 1.5	35.4 ± 4.4	6.2 ± 2.8	0.01 ± 0.03
Nov. 2011	22.9	77.0	28.3	27.1 ± 11.6	5.8 ± 5.0	6.2 ± 2.8	8.1 ± 5.3	6.7 ± 6.5	30.5 ± 9.8	8.3 ± 5.0	7.3 ± 8.6
Dec. 2011	16.4	64.3	39.2	18.5 ± 8.6	3.2 ± 2.0	6.7 ± 1.7	17.1 ± 4.9	1.4 ± 0.2	45.0 ± 7.0	6.8 ± 2.4	1.4 ± 1.6
Jan. 2012	14.4	80.3	29.7	10.4 ± 9.9	8.5 ± 6.3	1.0 ± 1.1	27.5 ± 9.5	3.8 ± 5.1	43.9 ± 18.4	3.6 ± 4.8	1.3 ± 2.2
Feb. 2012	14.9	84.2	29.7	15.9 ± 9.9	10.3 ± 8.0	3.9 ± 5.2	29.3 ± 9.1	5.8 ± 9.5	27.7 ± 6.2	5.1 ± 5.5	1.9 ± 1.5
*Spring 2011	21.2	75.3	33.8	34.9 ± 14.4	5.4 ± 4.1	16.6 ± 11.8	10.3 ± 7.6	10.9 ± 15.1	9.5 ± 7.3	7.6 ± 5.3	4.8 ± 4.5
*Summer 2011	28.3	79.0	18.0	28.2 ± 23.0	14.0 ± 21.3	6.1 ± 7.0	1.8 ± 3.6	24.7 ± 20.3	6.6 ± 7.6	10.7 ± 6.7	7.9 ± 6.1
*Fall 2011	25.0	78.1	28.8	35.3 ± 12.9	4.4 ± 4.6	5.0 ± 2.1	6.5 ± 5.1	6.2 ± 5.7	31.6 ± 7.7	7.1 ± 4.3	3.9 ± 8.8
*Winter 2012	16.4	75.8	34.1	20.9 ± 13.7	7.4 ± 6.1	5.3 ± 4.5	22.0 ± 10.9	3.8 ± 6.4	31.9 ± 14.9	5.6 ± 5.1	3.0 ± 2.9
Year	22.7	77.2	27.9	27.8 ± 18.1	8.9 ± 13.5	7.4 ± 8.0	11.0 ± 11.5	12.4 ± 16.5	19.5 ± 16.1	7.9 ± 5.9	5.1 ± 5.8

* The seasons are defined as: mid-Mar to mid-May as spring, mid-May to mid-Sep. as summer, mid-Sep. to mid-Nov. as fall, and mid-Nov. to mid-Mar. as winter.

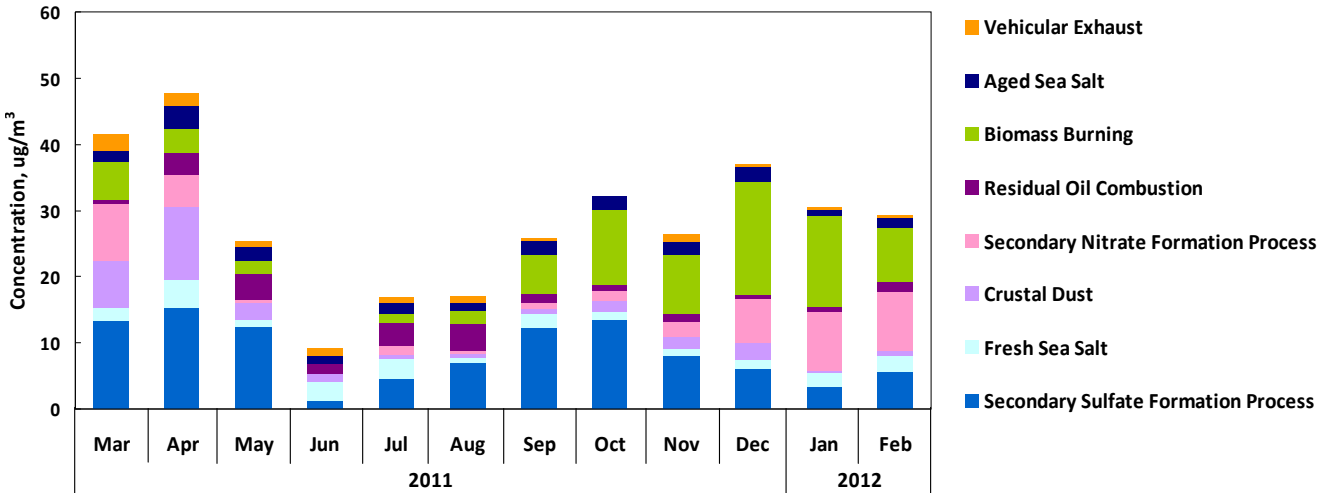

Fig. 9. The monthly source contributions to $PM_{2.5}$ observed at HKUST AQRS during Mar. 2011–Feb. 2012.

suggesting that the air quality meets the Hong Kong's proposed AQOs for most of the time in the suburban area of Hong Kong. In spite of this, there were several sampling days on which relatively high $PM_{2.5}$ concentrations were observed. The average and standard deviation of the $PM_{2.5}$ concentrations were calculated from all the individual sampling days. Samples with the daily $PM_{2.5}$ concentrations higher than the average value plus one standard deviation (44.0 μg/m^3) are defined as high PM days (denoted by "high" hereinafter) while those with daily $PM_{2.5}$ concentrations lower than the average value minus one standard deviation (11.7 μg/m^3) are referred to low PM days (denoted by "low"). There are 16 high PM days and 18 low PM days by these criteria for PM levels.

Fig. 10(a) demonstrates the average reconstructed mass for the high and low PM days defined as above. On high PM days, the increased mass consists of all the major components. This is because that the HKUST AQRS is located in an area where significant sources in the immediate neighborhood of a few kilometers are relatively limited so that majority of the pollutants were very likely transported from distant urban areas. The PMF-derived source contributions were also averaged for these two scenarios (Fig. 10(b)) and it can be seen that local sources of residual oil combustion, fresh sea salt, and vehicular exhaust were more dominant (75.6%) on low PM days. On the other hand, biomass burning, secondary sulfate and nitrate formation processes made significant contributions (85.7%) on high PM days, suggesting that the increased PM mass should be associated with transport of air pollutants from the regions outside Hong Kong. Results from this study indicate the necessity of regional/super-regional strategies for reducing $PM_{2.5}$ in Hong Kong.

CONCLUSIONS

A $PM_{2.5}$ sampling campaign was conducted at the HKUST Air Quality Research Supersite from March 2011 to February 2012. 24-hr $PM_{2.5}$ filter samples were collected using both high-volume and mid-volume samplers. Samples on a total of 83 sampling days were subjected to chemical analyses including major ions, organic carbon, elemental carbon, elements, and non-polar organic compounds. Three levels of data validation procedures were performed to obtain the valid dataset.

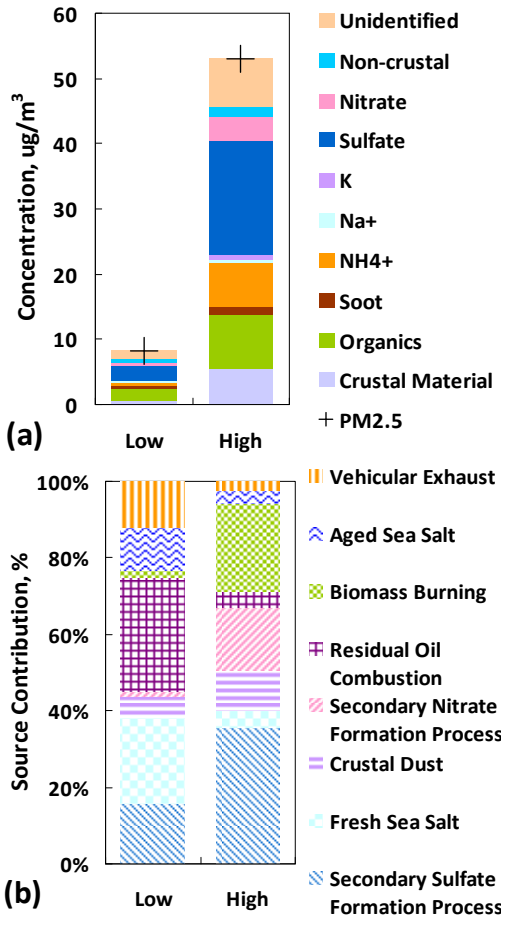

Fig. 10. (a) Average reconstructed mass and (b) relative source contributions for the high and low PM days at HKUST AQRS during Mar. 2011–Feb. 2012.

The sum of crustal materials, organic matter, soluble sodium, ammonium, potassium, sulfate, nitrate, and non-crustal trace elements could explain approx. 90% of the measured mass. Overall, sulfate is the most abundant component in the $PM_{2.5}$ mass, followed by organic matter and ammonium. As a suburban sampling site with little commercial and residential development, most of the pollutants observed at HKUST AQRS were transported from other areas. Different monthly variation patterns were observed for different components, reflecting variable regional/super-regional sources as a result of variation in synoptic weather conditions. The contribution by crustal materials was greater in March and April than in other months, which is believed to be associated with the dust storms originating from Northern China. Nitrate made more significant contributions in winter months due to its temperature-dependent formation or/and regional/super-regional transport of the air pollutants.

PMF analysis was conducted on the valid dataset and an eight-factor solution was adopted. The relative contributions by various sources to the $PM_{2.5}$ mass were estimated on a monthly, seasonal, and annual basis. In general, secondary sulfate formation process, biomass burning, and secondary nitrate formation process have been the dominant contributing sources throughout the sampling year. The monthly and seasonal variations of the source contributions suggest that sources including secondary sulfate and nitrate formation processes, biomass burning and crustal dust would mainly come from regions outside Hong Kong (non-local) while fresh sea salt, residual oil combustion, and vehicle exhaust are more likely emission sources within the local Hong Kong region. On an annual basis, non-local sources accounted for 66% of the $PM_{2.5}$ concentrations observed at the HKUST AQRS while local sources accounted for the other 34%.

Of the 83 individual sampling days, 43 daily samples were with $PM_{2.5}$ mass concentrations exceeding the WHO health standards (25 $\mu g/m^3$) and none were found exceeding the AQOs standard recently proposed by the Hong Kong government (75 $\mu g/m^3$). The major chemical composition and the contributing sources were examined for the high and low PM days. The increasing masses of all the major components on high PM days again confirmed that the major portion of the pollutants observed at HKUST AQRS was transported from elsewhere. PMF analysis showed that sources including biomass burning, secondary sulfate and nitrate formation processes, which are all associated with regional/super-regional air pollutant transport from non-local areas, contributed significantly to the $PM_{2.5}$ mass on high PM days.

ACKNOWLEDGEMENTS

This work is supported by the Environment and Conservation Fund/Woo Wheelock Green Fund (ECWW09EG04) and Hong Kong Environment Protection Department (HKEPD) (AS 10-131). We thank Hong Kong University Grant Council Special Equipment Grant (SEG HKUST07) for making RT-ECOC measurements possible and HKEPD for provision of the MARGA and real-time $PM_{2.5}$ datasets. The content of this paper does not necessarily reflect the views and policies of the HKSAR Government, nor does mention of trade names or commercial products constitute an endorsement or recommendation of their use.

REFERENCES

Andreae, M.O. and Crutzen, P.J. (1997). Atmospheric Aerosols: Biogeochemical Sources and Role in Atmospheric Chemistry. *Science* 276: 1052–1058.

Chow, J.C. and Watson, J.G. (1998). Guideline on Speciated Particulate Monitoring, Third Draft Report Prepared for U.S. Environmental Protection Agency, Office of Air Quality Planning and Standards, Research Triangle Park, NC, by Desert Research Institute, Reno, NV.

Chow, J.C. and Watson, J.G. (2002). Review of $PM_{2.5}$ and PM_{10} Apportionment of Fossil Fuel Combustion and Other Sources by Chemical Mass Balance Receptor Model. *Energy Fuels* 16: 222–260.

Eldred, R.A., Cahill, T.A. and Feeney, P.J. (1987). Particulate Monitoring at US National Parks Using PIXE. *Nucl. Instrum. Methods Phys. Res., Sect. B* 22: 289–295.

Hagler, G.S.W., Bergin, M.H., Salmon, L.G., Yu, J.Z., Wan, E.C., Zheng, H.M., Zeng, L.M., Kiang, C.S., Zhang, Y.H., Lau, A.K.H. and Schauer, J.J. (2006). Source Areas and Chemical Composition of Fine Particulate Matter in the Pearl River Delta Region of China. *Atmos. Environ.* 40: 3802–3815.

HKEPD (Hong Kong Environmental Protection Department) (2013). 2011 Hong Kong Emission Inventory Report. Available at: http://www.epd.gov.hk/epd/english/environmentinhk/air/data/files/2011HKEIReport.pdf.

Ho, K.F., Lee, S.C., Chan, C.K., Yu, J.Z., Chow, J.C. and Yao, X.H. (2003). Characterization of chemical species in $PM_{2.5}$ and PM_{10} aerosols in Hong Kong. *Atmos. Environ.* 37: 31–39.

Ho, S.S.H., Yu, J.Z., Chow, J.C., Zielinska, B., Watson, J.G., Sit, E.H.L. and Schauer, J.J. (2008). Evaluation of an In-Injection Port Thermal Desorption-Gas Chromatography Mass Spectrometry Method for Analysis of Non-Polar Organic Compounds in Ambient Aerosol Samples. *J. Chromatogr. A* 1200: 217–227.

Hong Kong Observatory (2013). Climate of Hong Kong, Climatological Information Services, Available at: http://www.hko.gov.hk/cis/climahk_e.htm.

Kanakidou, M., Seinfeld, J.H., Pandis, S.N., Barnes, I., Dentener, F.J., Facchini, M.C., Van Dingenen, R., Ervens, B., Nenes, A., Nielsen, C.J., Swietlicki, E., Putaud, J.P., Balkanski, Y., Fuzzi, S., Horth, J., Moortgat, G.K., Winterhalter, R., Myhre,C.E.L., Tsigaridis, K., Vignati, E., Stephanou, E.G. and Wilson, J. (2005). Organic Aerosol and Global Climate Modeling: A Review. *Atmos. Chem. Phys.* 5: 1053–1123.

Kavouras, I.G., Stratigakis, N. and Stephanou, E.G. (1998). Iso- and Anteiso-Alkanes: Specific Tracers of Environmental Tobacco Smlke in Indoor and Outdoor Particle-Size Distributed Urban Aerosol. *Environ. Sci. Technol.* 32: 1369–1377.

Kowalczyk, G.S., Gordon, G.E. and Rheingrover, S.W. (1982). Identification of Atmospheric Particulate Sources in Washington D.C. Using Chemical Element Balances. *Environ. Sci. Technol.* 16: 79–90.

Louie, P.K.K., Chow, J.C., Chen, L.W.A., Watson, J.G., Leung, G. and Sin, D.W.M. (2005a). $PM_{2.5}$ Chemical Composition in Hong Kong: Urban and Regional Variations. *Sci. Total Environ.* 338: 267–281.

Louie, P.K.K., Watson, J.G., Chow, J.C., Chen, A., Sin, D.W.M. and Lau, A.K.H. (2005b). Seasonal Characteristics and Regional Transport of $PM_{2.5}$ in Hong Kong. *Atmos. Environ.* 39: 1695–1710.

Malm, W.C., Sisler, J.F., Huffman, D., Eldred, R.A. and Cahill, T.A. (1994). Spatial and Seasonal Trends in Particle Concentration and Optical Extinction in the United States. *J. Geophys. Res.* 99: 134701370.

Norris, G., Vedantham, R., Wade, K., Brown, S., Prouty, J., Foley, C. and Martin, L. (2008). EPA Positive Matrix (PMF) 3.0 Fundamentals & User Guide, U.S. Environmental Protection Agency.

Novakov, T. and Penner, J.E. (1993). Large Contribution of Organic Aerosols to Cloud-Condenstaion-Nuclei Concentrations. *Nature* 365: 823–826.

Polissar, A.V., Hopke, P.K., Zhou, L., Paatero, P., Park, S.S. and Ondov, J.M. (1998). Atmospheric Aerosol over Alaska 2. Elemental Composition and Sources. *J. Geophys. Res.* 103: 19045–19057.

Qin, Y., Chan, C.K. and Chan, L.Y. (1997). Characteristics of Chemical Compositions of Atmospheric Aerosols in Hong Kong: Spatial and Seasonal Distributions. *Sci. Total Environ.* 206: 25–37.

Ramanathan, V., Crutzen, P.J., Kiehl, J.T. and Rosenfeld, D. (2001). Atmosphere: Aerosol, Climate, and the Hydrological Cycle. *Science* 294: 2119–2124.

Reff, A., Eberly, S.I. and Bhave, P.V. (2007). Receptor Modeling of Ambient Particulate Matter Data Using Positive Matrix Factorization: Review of Existing Methods. *J. Air Waste Manage. Assoc.* 57: 146–154.

Roberts, G.C., Andreae, M.O., Zhou, J. and Artaxo, P. (2001). Cloud Condensation Nuclei in the Amazon Basin: "Marine" Conditions over a Continent? *Geophys. Res. Lett.* 28: 2807–2810.

Rogge, W.F., Hildemann, L.M., Mazurek, M.A. and Cass, G.R. (1994). Sources of Fine Organic Aerosol. 6. Cigarette Smoke in the Urban Atmosphere. *Environ. Sci. Technol.* 28: 1375–1388.

Saxena, P. and Hildemann, L.M. (1996). Water-Soluble Organics in Atmospheric Particles: a Critical Review of the Literature and Application of Thermodynamics to Identify Candidate Compounds. *J. Atmos. Chem.* 24: 57–109.

Schauer, J.J., Kleeman, M.J., Cass, G.R. and Simoneit, B.R.T. (1999). Measurement of Emissions from Air Pollution Sources. 2. C_1 Through C_{30} Organic Compounds from Medium Duty Diesel Trucks. *Environ. Sci. Technol.* 33: 1578–1587.

Schauer, J.J., Kleeman, M.J., Cass, G.R. and Simoneit, B.R.T. (2002). Measurement of Emissions from Air Pollution Sources. 5. C_1–C_{32} Organic Compounds from Gasoline-Powered Motor Vehicles. *Environ. Sci. Technol.* 36: 1169–1180.

Schauer, J.J., Mader, B.T., DeMinter, J.T., Geidemann, G., Bae, M.S., Seinfeld, J.H., Flagan, R.C., Cary, R.A., Smith, D., Huebert, B.J., Bertram, T., Howell, S., Kline, J.T., Quinn, P., Bates, T., Turpin, B., Lim, H.J., Yu, J.Z., Yang, H. and Keywood, M.D. (2003). ACE-Asia Intercomparison of a Thermal-Optical Method for the Determination of Particle-Phase Organic and Elemental Carbon. *Environ. Sci. Technol.* 37: 993–1001.

So, K.L., Guo, H. and Li, Y.L. (2007). Long-Term Variation of $PM_{2.5}$ Levels and Composition at Rural, Urban, and Roadside Sites in Hong Kong: Increasing Impact of Regional Air Pollution. *Atmos. Environ.* 41: 9427–9434.

Subramanian R., Donahue, N.M., Bernardo-Bricker, A., Rogge, W.F. and Robinson, A.L. (2006). Contribution of Motor Vehicle Emissions to Organic Carbon and Fine Particle Mass in Pittsburgh, Pennsylvania: Effects of Varying source Profiles and Seasonal Trends in Ambient Marker Concentrations. *Atmos. Environ.* 40:8002–8019.

Putaud, J., Raes, F., Van Dingenen, R., Brüggemann, E., Facchini, M.C., Decesari, S., Fuzzi, S., Gehrig, Ro, Hüglin, C., Laj, P., Lorbeer, G., Maenhaut, W., Mihalopoulos, N., Müller, K., Querol, X., Rodriguez, S., Schneider, J., Spindler, G., Brink, H. ten, Tørseth, K. and Wiedensohler, A. (2004). A European Aerosol Phenomenology - 2: Chemical Characteristics of Particulate Matter at Kerbside, Urban, Rural and Background Sites in Europe. *Atmos. Environ.* 38: 2579–2595.

USEPA (1999). Particulate Matter ($PM_{2.5}$) Speciation Guidance, Final Draft.

Watson, J.G. (2002). Visibility: Science and Regulation. *J. Air. Waste. Manage. Assoc.* 52: 628–713.

World Health Organization (2006). WHO Air Quality Guidelines for Particulate Matter, Ozone, Nitrogen Dioxide and Sulfur Dioxide: Global Update 2005. Available at http://whqlibdoc.who.int/hq/2006/WHO_SDE_PHE_OEH_06.02_eng.pdf.

Wu, C.W. Ng, M., Huang, J.X., Wu, D. and Yu, J.Z. (2012). Determination of Elemental and Organic Carbon in $PM_{2.5}$ in the Pearl River Delta Region: Inter-instrument (Sunset vs. DRI Model 2011 Thermal/Optical Carbon Analyzer) and Inter-Protocol Comparisons (IMPROVE vs. ACE-Asia Protocol). *Aerosol Sci. Technol.* 46: 610–621.

Yu, J.Z., Huang, X.H.H., Ho, S.S.H. and Bian, Q.J. (2012). Nonpolar Organic Compounds in Fine Particles: Quantification by Thermal Desorption–GC/MS and Evidence for Their Significant Oxidation in Ambient Aerosols in Hong Kong. *Anal. Bioanal.Chem.* 401: 3125–3139.

Yuan, Z. B., Yadav, V., Turner, J.R., Louie, P.K.K. and Lau, A.K.H. (2012). Long-Term Trends of Ambient Particulate Matter Emission Source Contributions and the Accountability of Control Strategies in Hong Kong over 1998–2008. *Atmos. Environ.* 76: 21–31.

Zhang, Q., Jimenez, J.L., Canagaratna, M.R., Allan, J.D., Coe, H., Ulbrich, I., Alfarra, M.R., Takami, A., Middlebrook, A.M., Sun, Y.L., Dzepina, K., Dunlea, E.,

Docherty, K., DeCarlo, P.F., Salcedo, D., Onasch, T., Jayne, J.T., Miyoshi, T., Shimono, A., Hatakeyama, S., Takegawa, N., Kondo, Y., Schneider, J., Drewnick, F., Borrmann, S., Weimer, S., Demerjian, K., Williams, P., Bower, K., Bahreini, R., Cottrell, L., Griffin, R.J., Rautiainen, J., Sun, J.Y., Zhang, Y.M. and Worsnop, D.R. (2007). Ubiquity and Dominance of Oxygenated Species in Organic Aerosols in Anthropogenically-Influenced Northern Hemisphere Midlatitudes. *Geophys. Res. Lett.* 34: L13801, doi: 10.1092/2007GL029979.

Zheng, J., Zhang, L., Che, W., Zheng, Z. and Yin, S. (2009). A Highly Resolved Temporal and Spatial Air Pollutant Emission Inventory for the Pearl River Delta Region, China and Its Uncertainty Assessment. *Atmos. Environ.* 43: 5112–5122.

Received for review, January 22, 2013
Accepted, June 25, 2013